

Earthquake Response of Idealized Twenty Story Buildings
Having Various Elasto-Plastic Properties

by

Toshihiko Hisada*, Kyoji Nakagawa* and Masanori Izumi*

Synopsis

Systematic analyses on earthquake response of twenty-story R.C. and steel buildings by digital electronic computations are presented. Idealized shear beam type models having various distributions of rigidity and restoring force characteristics in elastic and elasto-plastic ranges are assumed, and their response to the El Centro and Taft earthquakes with differing assumed ranges of intensities were computed. The analytical results obtained would serve for the earthquake resistant design of this type of structure.

Notations

A_i = Relative acceleration of i th floor to the base (= \ddot{y}_i)
 C_i = Damping coefficient of i th floor
 K_i = Spring constant at i th floor
 M_i = Overturning Moment at the foot of i th floor
 Q_i = Restoring force at i th floor
 Q_{yi} = Yield shearing force
 s^T = Undamped natural period of s th mode
 a_i = Relative acceleration of i th floor to $i-1$ th floor (= $A_i - A_{i-1}$)
 $c_i = C_i/m_i$
 d_i = Relative displacement of i th floor to $i-1$ th floor (= $y_i - y_{i-1}$)
 s^h = Fraction of critical damping of s th mode
 i = Number of floor from the base
 j = Time step counted from the beginning of an earthquake motion
 m_i = Mass of i th floor
 $q_i = Q_i/m_i$
 $q_{yi} = Q_{yi}/m_i$
 r = Ratio of slope (= θ_2/θ_1 , see Fig. 1 b)
 $u_{i+1} = m_{i+1}/m_i$
 v_i = Relative velocity of i th floor to $i-1$ th floor (= $\dot{y}_i - \dot{y}_{i-1}$)
 y_i = Relative displacement of i th floor to the base
 $\alpha(t)$ = Ground acceleration (= \ddot{y}_0)
 μ_i = Ductility factor at i th floor
 μ_i' = Imaginary ductility factor at i th floor in linear response
 τ = Fragment of time

Idealized Dynamic Models of Building Structures

Sets of dynamic models for the buildings are selected as follows;

- (1) Shear buildings of 20 stories having equal mass at each floor and fixed support at their bases are adopted. Therefore, they are serial mass-spring systems having 20 degrees of freedom as shown in Fig. 1 a.

* Building Research Institute, Ministry of Construction

- (2) Two types of buildings, reinforced concrete building (I) and steel building (II), are assumed with fundamental natural periods T_1 of 1.4 sec. and 2.0 sec. respectively.
- (3) Distribution of rigidity, or distribution of spring constant K_i is linear from the top K_T to the bottom K_B . The ratio of K_T to K_B is varied in steps of 1/3, 1/5, 1/7, 1/10 for the building I, and 1/2, 1/3, 1/5, 1/7 for the building II. The natural periods in higher modes are calculated as shown in Table 2.
- (4) The relation between interstory deflection d_i and restoring force Q_i is assumed bi-linear as shown in Fig. 1 b. The yield points of the bi-linear systems are determined as follows:
The yield deflections at the 10 th floor d_{y10} are assumed to be 0.7 cm (1/500 story height) in the R.C. structure and 1.17 cm (1/300 story height) in the steel structure in the case of $K_T/K_B = 1/7$. Values of yield shearing force Q_{yi} are obtained from the equation $Q_{yi} = \beta K_i^{3/4}$, where β is calculated from the above assumptions.
- (5) Damping is assumed so that the fraction of critical damping ζ_1 of the first mode in linear vibration is 5%. Besides, the damping coefficient C_i takes the following relation, in order to satisfy the principal vibration.

$$C_i = \frac{1T_1h}{\pi} \cdot K_i$$

C_i takes a constant value during the vibrational motion along bi-linear restoring force characteristics.

- (6) The value of r , the ratio of the slope after the yield point to that before is so given as 1.0 (linear), 0.1, 0 or -0.05. (See Fig. 1 b)

Earthquake Motions as Input Data

Acceleration records of three earthquakes shown in Table 1 were used, and their amplitudes were adjusted so that the maximum value of each earthquake is equal to that of the El Centro Earthquake (0.33g). Additionally, in order to find out the effect of the intensity, calculations were made for the earthquakes with changed acceleration amplitudes.

Digital values of the accelerations used in the calculations are those which were sent from Prof. G.L. Berg, Univ. of Michigan, U.S.A., to Prof. K. Muto, Univ. of Tokyo.

As the values of acceleration amplitudes obtained by linear interpolation for the equal interval of 0.01 sec. were used, some of the peak values could be missed, but the interval is so short that large errors might not be expected. The durations of the earthquakes were cut off and shortened as shown in Table 1.

Method of Analysis

The equation of motion of the i th mass of a multi-story shear building is written as follows. (See Fig. 1 a)

$$m_i \ddot{y}_i + C_i(\dot{y}_i - \dot{y}_{i-1}) - C_{i+1}(\dot{y}_{i+1} - \dot{y}_i) + Q_i - Q_{i+1} = -m_i \alpha(t)$$

$$A_i + c_i v_i - u_{i+1} c_{i+1} v_{i+1} + q_i - u_{i+1} q_{i+1} = -\alpha(t)$$

For numerical analysis of the above equation, the following relations are used:

$$v_{ij} = v_{ij-1} + \tau a_{ij-1} + \frac{\tau^2}{2} \dot{a}_{ij-1}$$

$$d_{ij} = d_{ij-1} + \tau v_{ij-1} + \frac{\tau^2}{2} a_{ij-1} + \frac{\tau^3}{6} \dot{a}_{ij-1}$$

Computations were carried out by an electronic digital computer NEAC 2230. Detailed programming is indicated in the reference paper (2) by the authors.

Besides the analyses made on the assumed models mentioned above, further studies were carried out to find the values of k_i for given distributions of μ'_i or d_i max.

Computed Results

- (1) The following values were computed for all systems of building I and building II, both in linear ($r = 1$) and non-linear ($r = 0.1, 0, -0.05$) response for three earthquakes.

- d_i max (μ_i max or μ'_i max)
- d_i for M_i max : Values of d_i at the time when respective i th story moment M_i becomes maximum.
- d_i for M_1 max : Values of d_i at the time when overturning moment at the base M_1 becomes maximum.
- y_i for M_1 max : Values of story deflection relative to the base at the time when M_1 becomes maximum.
- y_{20} max
- M_i max
- M_i for d_i max : M_i at the time when d_i becomes maximum.
- design O.M. : $\sum_{20}^i (Q_{yi} \times \text{story height})$

In these calculations, values of story height are assumed as unit (1 cm).

For example, Fig. 2 a, b show linear response of the building I ($K_T/K_B = 1/3$, $r = 1$) to the El Centro 40S Earthquake, and Figs. 3, 4 indicate non-linear response of the same system ($K_T/K_B = 1/3$, $r = 0.1$ and -0.05 respectively) to the same earthquake.

- (2) In Fig. 5 a, b, c, d, non-linear response of systems of building I ($K_T/K_B = 1/3, 1/5, 1/7$ and $1/10$, $r = 0$) to the El Centro 40S Earthquake are shown.
- (3) Fig. 6 a, b, c show the maximum values of interstory deflection at each floor of systems of the building I ($1T = 1.4$) to the El Centro 40S, Taft 52S and Taft 52W Earthquakes, where K_T/K_B of the systems are changed from $1/3$ to $1/10$. The design yield deflection d_{yi} and imaginary ductility factor μ'_i in linear response are also indicated in those Figures. As the

values of $d_{10 \max}$ remain almost constant throughout the change of K_T/K_B , relation between $d_i \max$ and K_T/K_B are compared for 3 earthquakes in Fig. 7.

The similar studies for systems of the building II ($T = 2.0$ sec.) are shown in Fig. 8 a, b, c and Fig. 9.

- (4) To study the effect of earthquake intensity, the El Centro 40S Earthquake was modified so that the maximum ground acceleration changes from 0.22g to 0.36g. The non-linear response of systems of the building I ($K_T/K_B = 1/7$ and $r = 0.1, 0, -0.05$) are plotted in Fig. 10 a, b, c. The effects of the intensity of the earthquake to M_{16}, M_{10}, M_1 are summarised in Fig. 11.
- (5) In Fig. 12, the values of $d_i \max$ and K_i of the R.C. structures ($T = 1.4$ sec.) having given distribution of u_i' ($u_i' = \text{const}$ and $u_T'/u_B' = 1.5/1$) are shown with the related design value of d_{yi}, Q_{yi} , story shear coefficient (S.C.) and linear response values of $d_i \max, Q_i \max$ and S.C. (See Systems I, II). For comparison, corresponding values of the building I with $K_T/K_B = 1/5$ are shown in the same figure. (See System III)

The same analyses were made for the steel structures ($T = 2.0$ sec.) and furthermore similar analysis under controlled uniform $d_i \max$ was also made. The results obtained are shown in Fig. 13.

Concluding Remarks

Based on the results of this analysis, the following conclusions are deduced:

- (1) Because periods of the idealized models for both R.C. and steel structures were kept constant, for various K_T/K_B (of 1/2 to 1/10) having linear variation of K_i , the value of K_{10} remains almost constant. Consequently as the values of K_T/K_B decrease, the maximum values of d_i ($d_i \max$) increase remarkably in the upper stories but decrease in the lower stories.
- (2) Provided u_i' is about 2 or less, the value of $d_i \max$ is almost proportional to the intensity of an earthquake, even in elasto-plastic response. $d_i \max$ is increased for negative values of r ($r = -0.05$), and decreased for positive values of r ($r = 0.1$) except at lower stories.
- (3) In both elastic and elasto-plastic response, M_i for $d_i \max$ is close in value to $M_i \max$. However, d_i at $M_i \max$ is smaller than $d_i \max$ particularly in the middle stories (see Figs. 2, 3 and 4). When the base moment, M_1 is a maximum, the mode has an inverted triangular shape, and the overturning moment at each story is close to the design values (see Figs. 2, 3 and 4).
- (4) Reasonable distributions of ductility factor up the building height in both elastic and elasto-plastic response can be expected, when the distribution of K_i is about $K_T/K_B = 1/5$ with K_i decreasing at the top (see Fig. 5).
- (5) The results of analysis for K_i under controlled distribution of u_i' in

elastic response meet the expectation mentioned above, although the values and distributions of K_i are not quite the same for respective earthquakes (see Figs. 12 and 13).

- (6) As there is an evident difference between the time when $d_{i \max}$ occurs in the upper and lower parts of the R.C. structures in the response to the El Centro Earthquake, discontinuity in the distribution of $d_{i \max}$ is observed. No such singular feature can be observed in response to the other earthquakes (see Figs. 2, 3, 4, 5 and 6 a).
- (7) In elastic response under controlled distribution of u'_i , the values of $d_{i \max}$ in steel structures are larger by about 20% to 60% than those in R.C. structures, depending on the earthquake (see Figs. 12 and 13).

References

1. T. Hisada, K. Nakagawa and M. Izumi, "Response of Tall Buildings Subjected to Strong Motion Earthquakes, Part I and Part II", Proceedings of Japan National Symposium on Earthquake Engineering, Nov. 1962.
2. T. Hisada, K. Nakagawa and M. Izumi, "Earthquake Response of Tall Buildings, Part I and Part II", Occasional Report, Building Research Institute, Ministry of Construction, 1964.

Table 1
Earthquake as Input Data

Earthquake	Date	Max. Ground Accel. (Actual)	Max. Ground Accel. (Calcu.)	Duration (Calculation)
E1 Centro 40S	May 18, 1940	0.33 g	0.33 g	8.0 sec.
Taft 52W	July 21, 1952	0.158 g	0.33 g	10.8 sec.
Taft 52S	July 21, 1952	0.178 g	0.33 g	11.8 sec.

Table 2
Natural Periods of Building I and Building II

	K_T/K_B	1^T	2^T	3^T	4^T	5^T
Building I	1/3	1.40 sec.	0.518	0.315	0.227	0.179
	1/5	1.40 sec.	0.542	0.332	0.240	0.189
	1/7	1.40 sec.	0.557	0.344	0.249	0.197
	1/10	1.40 sec.	0.574	0.357	0.260	0.205
Building II	1/2	2.00 sec.	0.713	0.432	0.311	0.244
	1/3	2.00 sec.	0.740	0.451	0.325	0.255
	1/5	2.00 sec.	0.774	0.475	0.343	0.270
	1/7	2.00 sec.	0.796	0.491	0.356	0.281

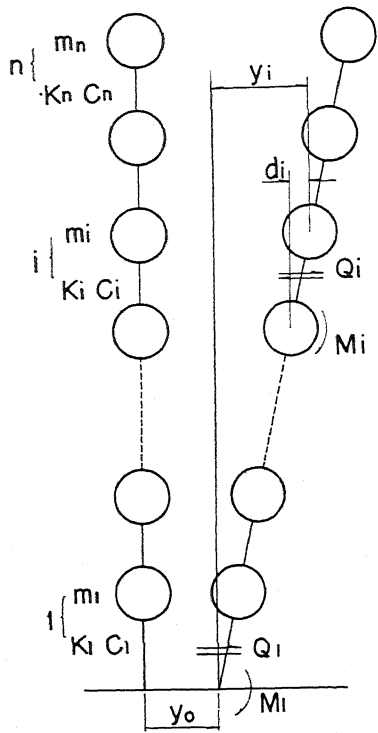


Fig. 1a Idealized Dynamical Model of Building

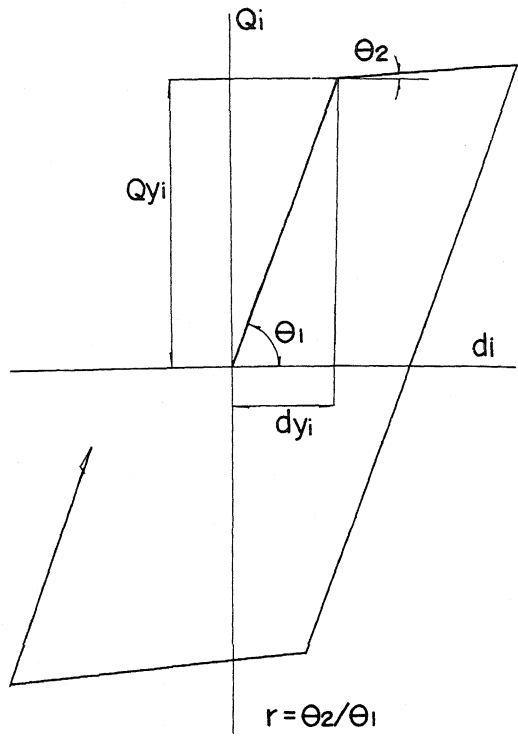


Fig. 1b Idealized Restoring Force - Displacement Characteristic in i th Story

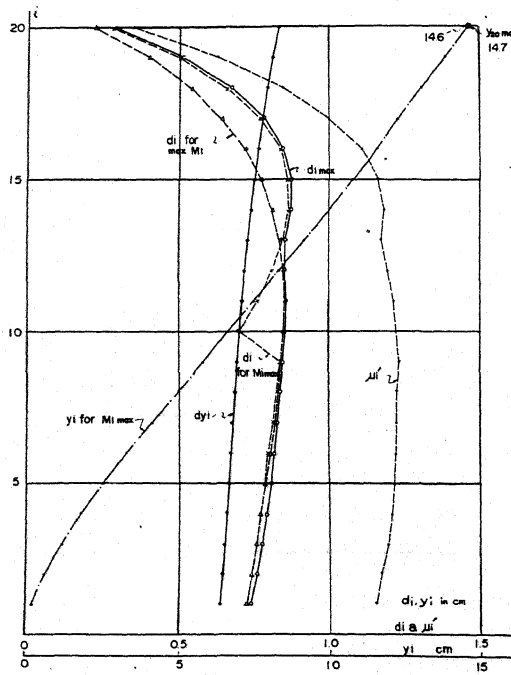


Fig. 2a Linear Response of Building I ($K_T/K_B = 1/3, r = 1.0$) to the E1 Centro 40S Earthquake (0.33g)

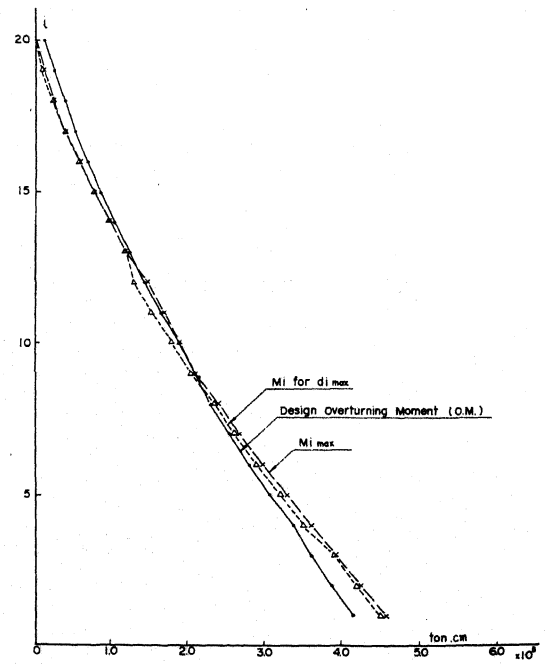


Fig. 2b Linear Response of Building I ($K_T/K_B = 1/3, r = 1.0$) to the E1 Centro 40S Earthquake (0.33g)

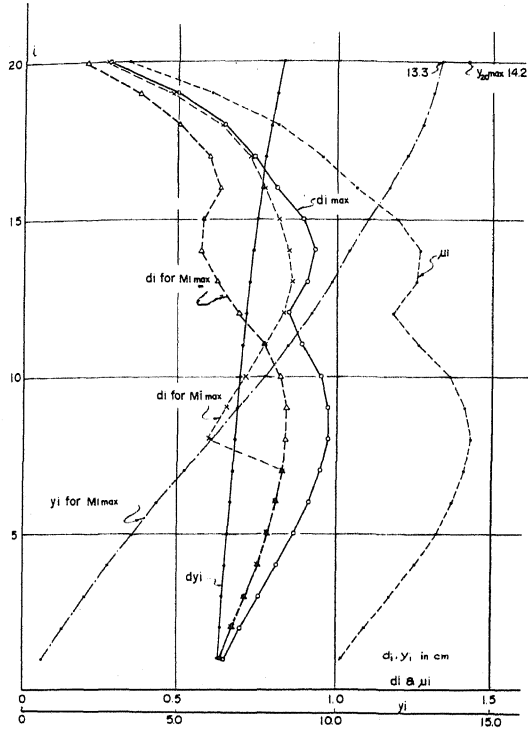


Fig. 3a Non-linear Response of Building I ($K_r/K_g = 1/3$, $r = 0.1$) to the El Centro 40S Earthquake (0.33g)

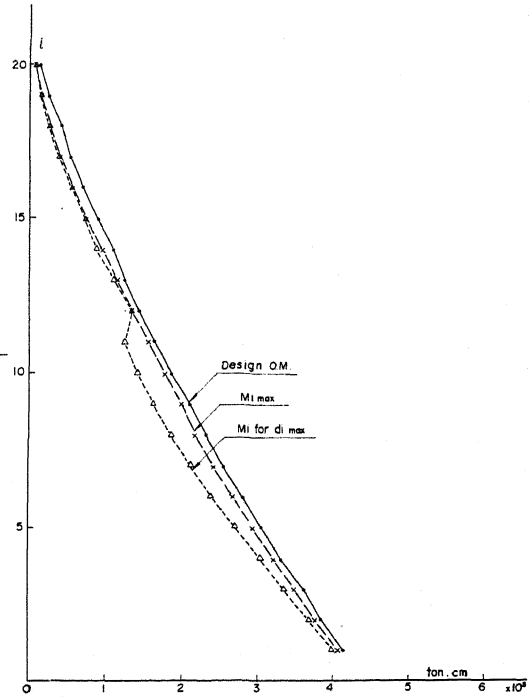


Fig. 3b Non-linear Response of Building I ($K_r/K_g = 1/3$, $r = 0.1$) to the El Centro 40S Earthquake (0.33g)

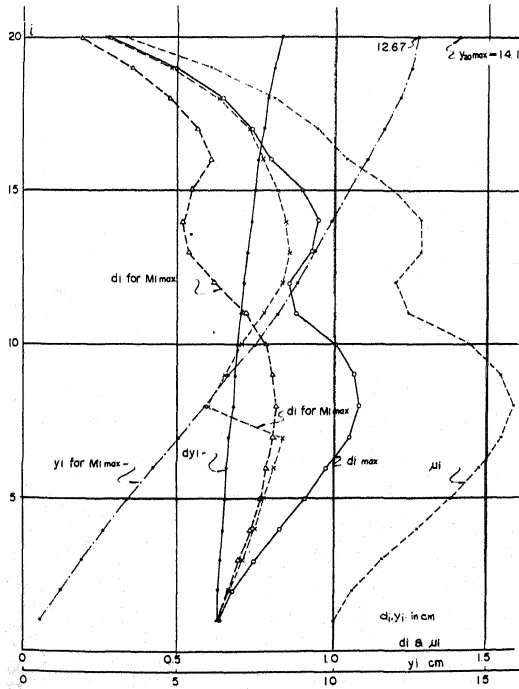


Fig. 4a Non-linear Response of Building I ($K_r/K_g = 1/3$, $r = -0.05$) to the El Centro 40S Earthquake (0.33g)

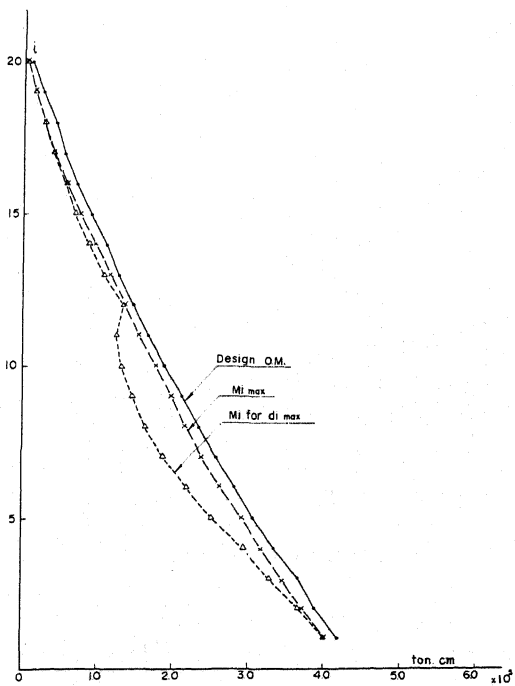


Fig. 4b Non-linear Response of Building I ($K_r/K_g = 1/3$, $r = -0.05$) to the El Centro 40S Earthquake (0.33g)

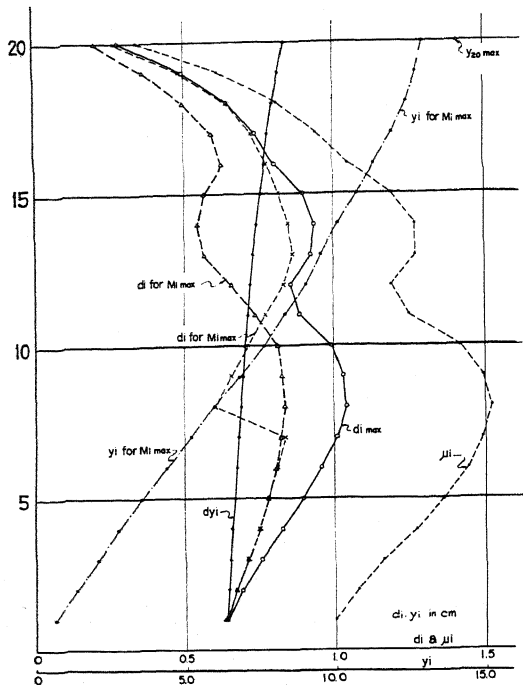


Fig. 5a Non-linear Response of Building I ($K_T/K_B = 1/3, c = 0$) to the El Centro 40S Earthquake (0.33g)

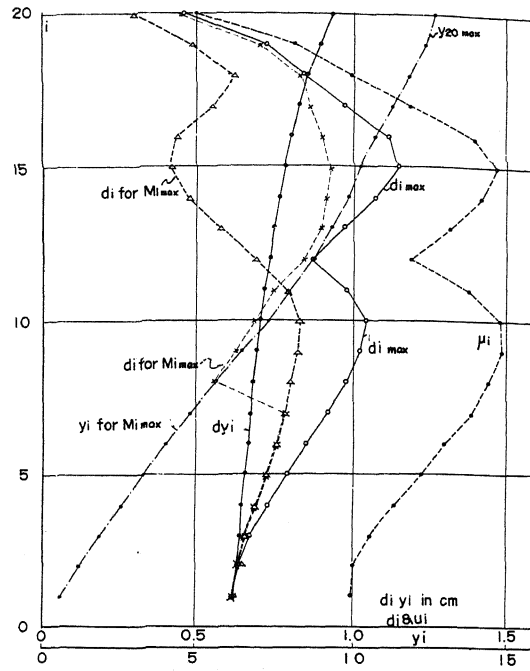


Fig. 5b Non-linear Response of Building I ($K_T/K_B = 1/5, c = 0$) to the El Centro 40S Earthquake (0.33g)

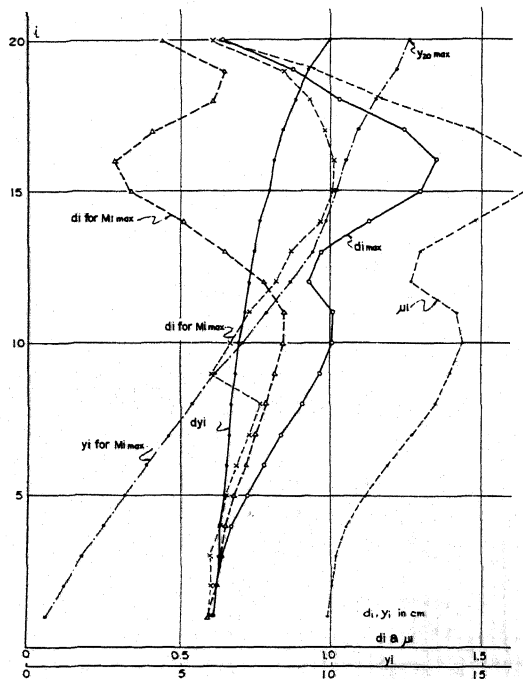


Fig. 5c Non-linear Response of Building I ($K_T/K_B = 1/7, c = 0$) to the El Centro 40S Earthquake (0.33g)

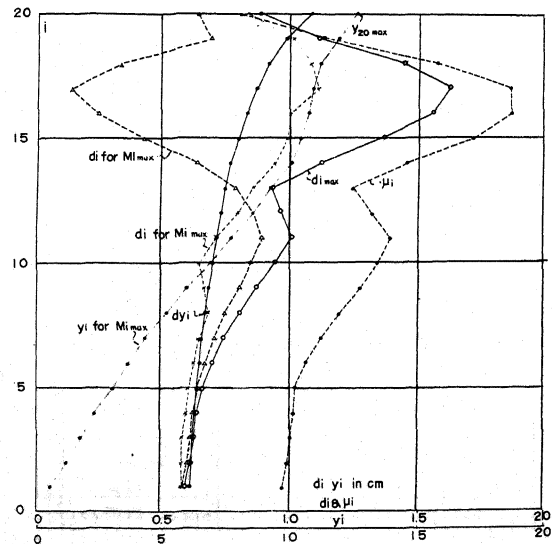


Fig. 5d Non-linear Response of Building I ($K_T/K_B = 1/10, c = 0$) to the El Centro 40S Earthquake (0.33g)

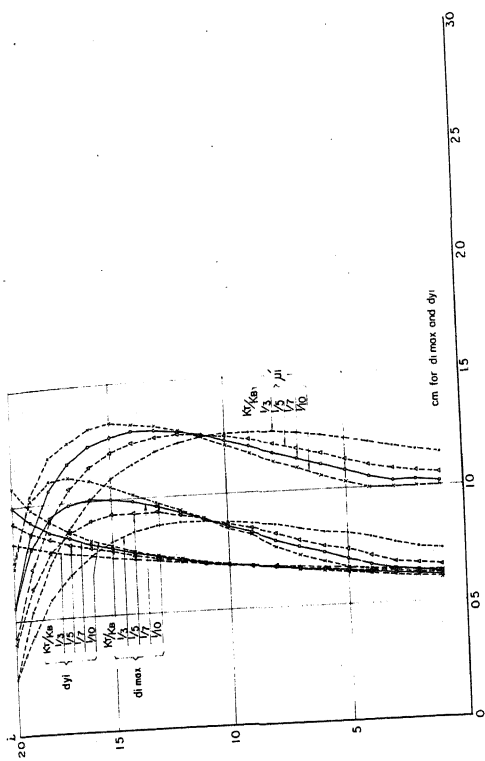


Fig. 6a Linear Response of Building I to the El Centro 40S Earthquake (0.33g)

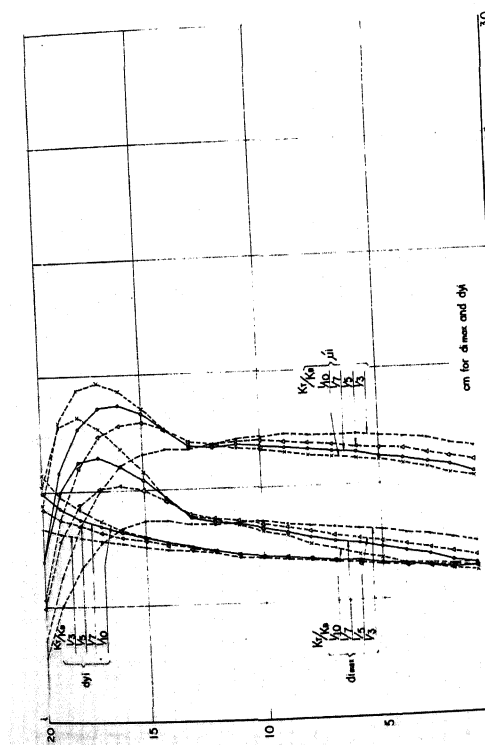


Fig. 6b Linear Response of Building I to the Taft 52S Earthquake (0.33g)

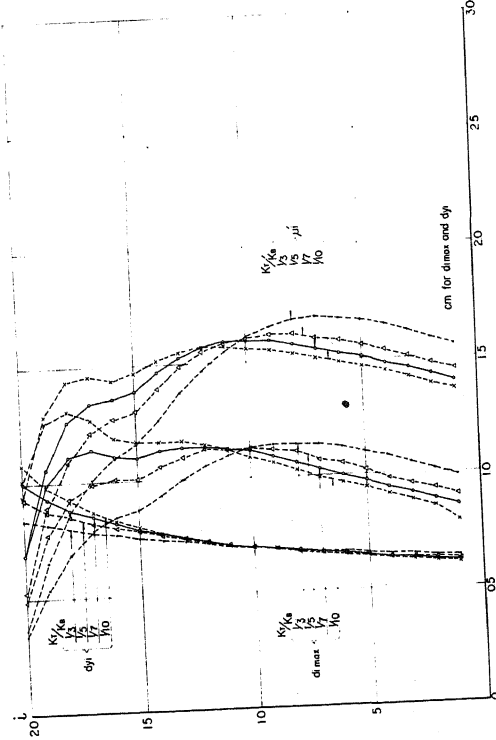


Fig. 6c Linear Response of Building I to the Taft 52W Earthquake (0.33g)

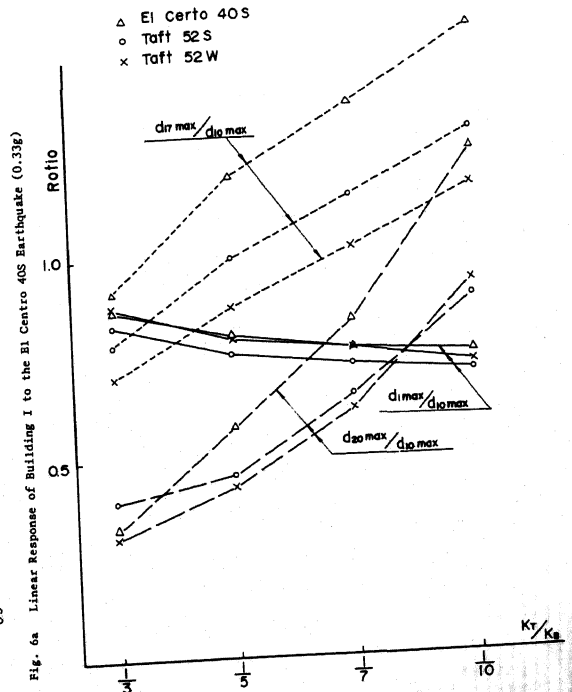


Fig. 7 Relation between $d_{1,max}/d_{10,max}$ and L_r/K_g in Linear Response of Building I to the El Centro 40S, Taft 52S and Taft 52W Earthquakes

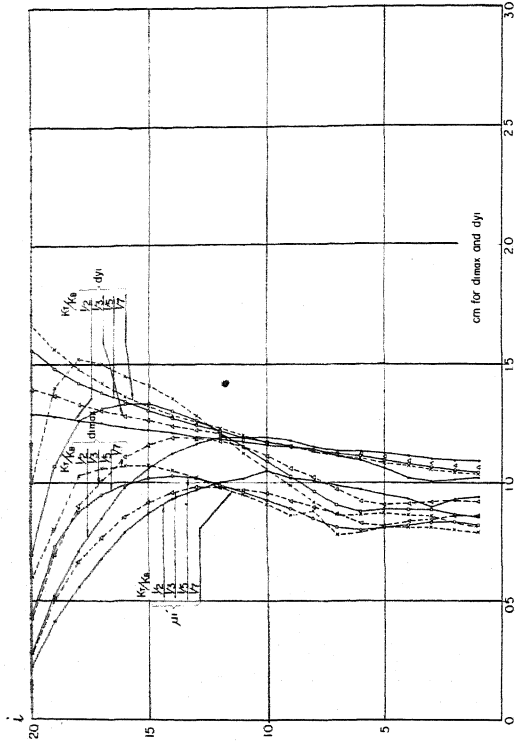


Fig. 8b Linear Response of Building II to the Taft 52S Earthquake (0.33g)

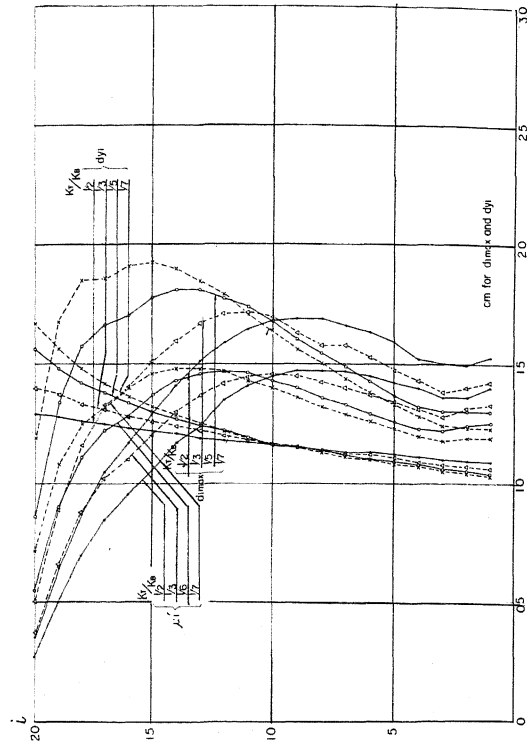


Fig. 8c Linear Response of Building II to the Taft 52W Earthquake (0.33g)

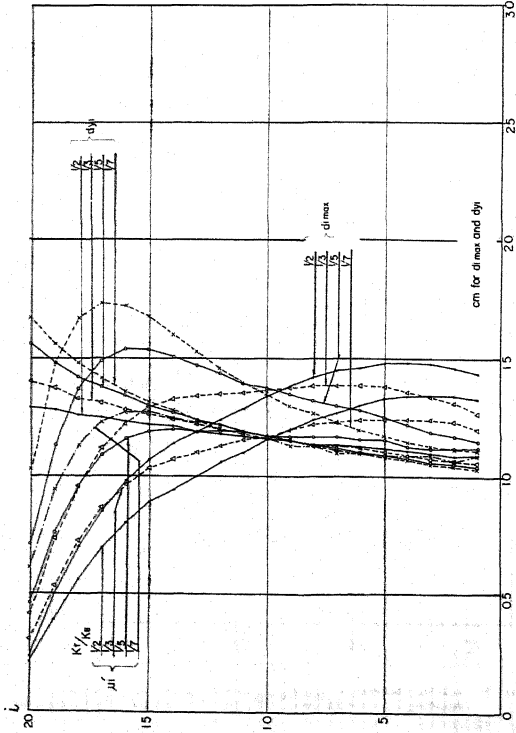


Fig. 8a Linear Response of Building II to the El Centro 40S Earthquake (0.33g)

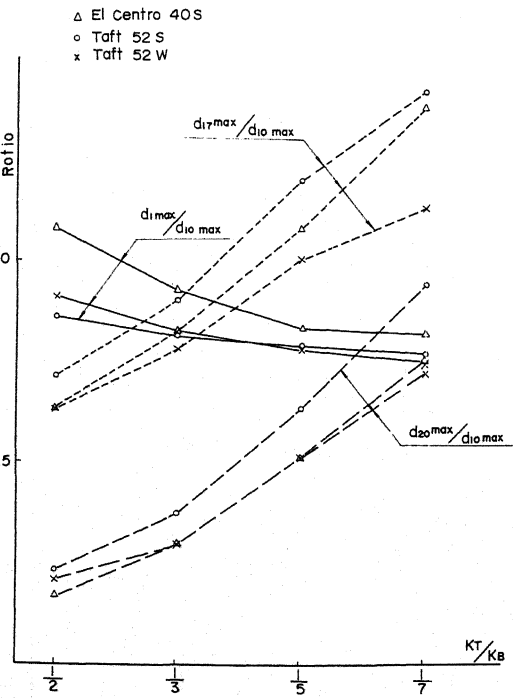


Fig. 9 Relation between $d_{i \max}/d_{10 \max}$ and K_t/K_b in Linear Response of Building II to the El Centro 40S, Taft 52S and Taft 52W Earthquakes

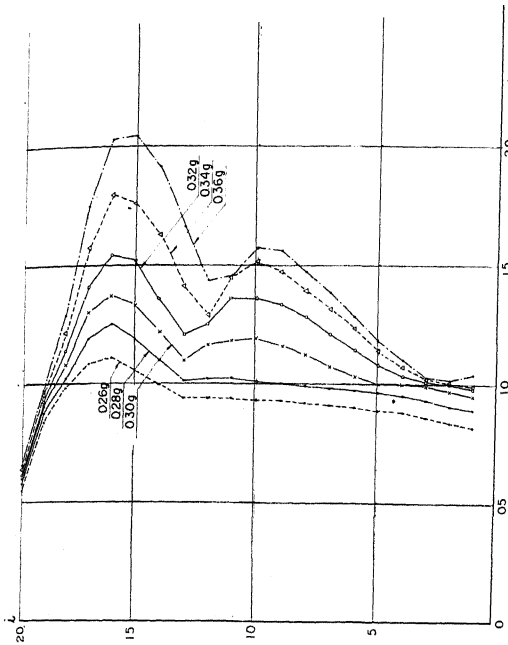


Fig. 10a Non-linear Response of Building I ($K_T/K_B = 1/7$, $r = 0.1$) to Various Intensities of the El Centro 40S Earthquake

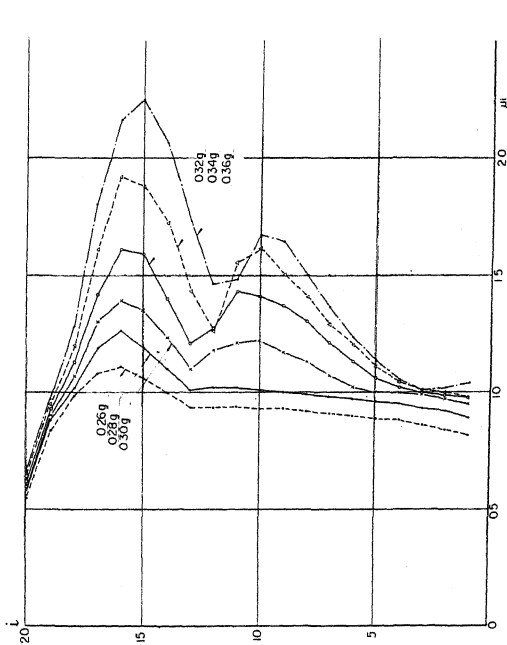


Fig. 10b Non-linear Response of Building I ($K_T/K_B = 1/7$, $r = 0$) to Various Intensities of the El Centro 40S Earthquake

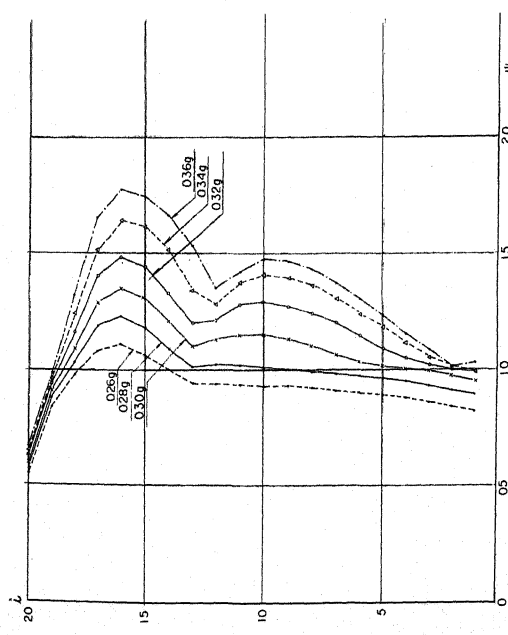


Fig. 10c Non-linear Response of Building I ($K_T/K_B = 1/7$, $r = -0.05$) to Various Intensities of the El Centro 40S Earthquake

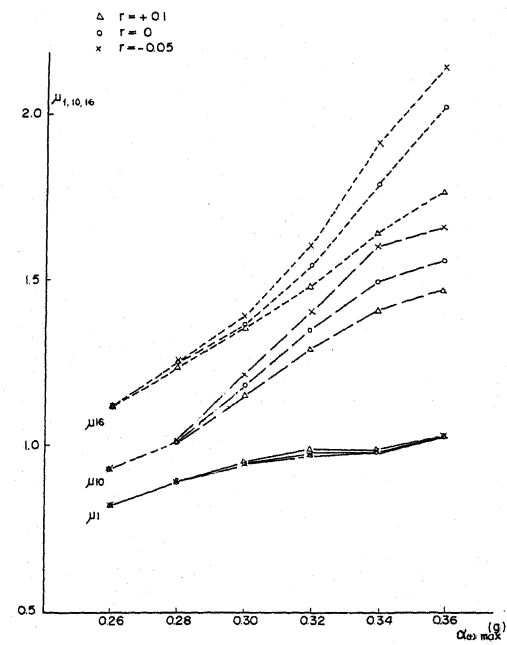


Fig. 11 Relation between $\mu_{1,10,16}$ of Building I ($K_T/K_B = 1/7$, $r = 0.1, 0, -0.05$) and Intensity of the El Centro 40S Earthquake

EARTHQUAKE RESPONSE OF IDEALIZED TWENTY STORY BUILDINGS HAVING VARIOUS
ELASTO-PLASTIC PROPERTIES

BY T.HISADA, K.NAKAGAWA AND M.IZUMI

QUESTIONS BY: R.W. CLOUGH - U.S.A.

1. The results of your paper are presented in terms of story ductility factors. How can you predict the ductility requirements in the individual columns and girders of the story?
2. Shear buildings, such as you have considered in your analysis, are assumed to have rigid girders, and all of the flexibility is contained in the columns. However, studies of both the elastic and the inelastic response of multistory frames show that the girder deformations can be quite large. Is it not likely that these girder deformations will have a significant effect on the dynamic behaviour of the structure, making it considerably different from the assumed shear building?

AUTHORS' REPLY: We think that the building can be regarded as a shear building as a whole for the ordinary range of the girder-deformations. On this supposition we made a macro-scopic study on the vertical distribution of rigidities. Therefore, such a problem as the yielding of individual columns and beams is not included in our study.

QUESTION BY: R.I. SKINNER - NEW ZEALAND

Would it be true to say that the building which you described could be represented by rigid floors and columns which allow the floors to move horizontally?

AUTHORS' REPLY: Our answer is "yes"

QUESTION BY: G.R. WALKER - NEW ZEALAND

At the University of Auckland in research on the transient response of two degree of freedom elasto-plastic systems, I have found that the distribution of lateral yield strength is the most critical factor in the distribution of ductility factor in the response.

AUTHORS' REPLY: As the yield strength of structures is not independent from their rigidities, we assume in this paper that the yield strength is proportional to the $3/4$

power of the rigidity. Therefore, no abrupt changes of strength exist and ductility factors gained from earthquake response are within a preferable range. We think the phenomenon suggested in your comment is expected when the yield strength is low and ductility factors are large.

QUESTION BY:

W.E. SAUL - U.S.A.

Since the material definition in Fig. 1b is unusual, could you clarify to which material it corresponds?

AUTHORS' REPLY:

Fig. 1b is widely used in seismic analyses to represent the idealized restoring force characteristics of steel and/or reinforced concrete structures.

QUESTION BY:

K.L. BENUSKA - U.S.A.

You have chosen to use a specialized form of damping which suppresses the higher mode response. If the system damping permitted larger response in the higher modes, for example, uniform damping of each mode, the story ductility factors would show a relative increase in the upper floors. The story ductility distribution would change in a manner similar to the stiffness-taper effect reported in the paper.

AUTHORS' REPLY:

As shown in the equation of motion, the inner-damping is assumed in this paper, which greatly affects the vibration of higher modes. According to the recent dynamic tests of buildings, damping for higher modes may not be so much assumed.

If so, as you point out, the dynamic behaviour of the upper part of buildings will be affected by the higher mode vibration. Though damping is a very important factor in dynamic problems, we have not obtained definite data about it.

QUESTION BY:

K. MUTO - JAPAN

You show in the last picture that the controlling story drift is 2cm and then you find how to arrange the stiffness and also the story height changes from 10 story to 20 story in that construction. I understand this study of story drift control method of designing and if you did control the story drift to 2 cm or $1/300$ th, then the curved stiffness elasticity becomes like the curved distribution of the picture. But in my studies of a 35 story building the stiffness distribution is not the same

as your result because in that case the story drift was controlled in only 2 cm and as a result in your curves the decrease is in the upper part but in our studies the stiffness distribution is not so nearly constant in the lower stories with a little decrease at the top. This was an ideal distribution for one example of design of a 35 storey building.

AUTHORS' REPLY: The interstorey deflections of a building in the response to given earthquakes can be controlled by adjusting the rigidities. When the drifts are uniformly controlled the vertical rigidity distribution takes a curve like a parabola. As the curve converges to a uniform value when the number of building storeys increase, then the 35 storey building has more uniform rigidity distribution than a 20 storey building in the deflection controlled systems. As for the details of the deflection controlled systems, please see the first volume of the Bulletin of IISEE in 1965.